On the relevant influence of limestone crystallinity on CO_2 capture in the Ca-looping technology at realistic calcination conditions

J. M. Valverde[a], P. E. Sanchez-Jimenez[b], L. A. Perez-Maqueda[b]

[a] Faculty of Physics. University of Seville. Avenida Reina Mercedes s/n, 41012 Sevilla, Spain

[b] Instituto de Ciencia de Materiales de Sevilla (C.S.I.C.–Univ. Seville), Americo Vespucio 49, 41092 Sevilla, Spain

Abstract

We analyze the role of limestone crystallinity on its CO_2 capture performance when subjected to carbonation/calcination cycles at conditions mimicking the Ca-looping (CaL) technology for post-combustion CO_2 capture. The behavior of raw and pretreated limestones (milled and thermally annealed) is investigated by means of thermogravimetric analysis (TGA) tests under realistic sorbent regeneration conditions, which necessarily involve high CO_2 partial pressure in the calciner and quick heating rates. The pretreatments applied lead to contrasting effects on the solid crystal structure and, therefore, on its resistance to solid-state diffusion. Our results show that decarbonation at high CO_2 partial pressure is notably promoted by decreasing solid crystallinity. CaO regeneration is fully achieved under high CO_2 partial pressure at 900°C in short residence times for the milled limestone whereas complete regeneration for raw limestone requires a minimum calcination temperature of about 950°C. Such a reduction of the calcination temperature and the mitigation of multicyclic capture capacity decay would serve to enhance the efficiency of the CaL technology. On the other hand, the results of our study suggest that the use of highly crystalline limestones would be detrimental since excessively high calcination temperatures should be required to attain full decarbonation.

I. INTRODUCTION

Pilot plants at the MW_{th} scale are currently demonstrating the feasibility of post-combustion CO_2 capture by means of the Ca-looping (CaL) technology based on the multicyclic carbonation/calcination of natural limestone derived CaO in dual fluidized bed reactors operated at atmospheric pressure [1, 2]. In this process, the flue gas is used to

fluidize a bed of CaO solid particles which, after being partially carbonated, are circulated into a second fluidized bed reactor where CO_2 is desorbed by calcination. Thus, the gas stream exiting the carbonator is almost free of CO_2 while a stream of highly concentrated CO_2 is released from the calciner, which is ready to be compressed and stored. The regenerated sorbent particles are then circulated back to the carbonator to be used in a new cycle. Values of operating parameters at practice are restricted by unavoidable constraints such as short gas-solid residence times (typically below 5 min), low CO_2 concentrations in the flue gas (typically around 15% vol) and high CO_2 concentration in the calciner (above 70% vol) [3]. Taking into account the tradeoff between the reaction kinetics and equilibrium, the optimum temperature for carbonation is around 650°C [1] whereas the minimum temperature for fast enough decarbonation to occur in the calciner under a high CO_2 partial pressure environment is close to 950°C [2–6]. In order to raise the temperature up to such a high value, the most practical method is to burn fuel in the calciner with pure oxygen, which serves to avoid CO_2 dilution. However, the production of SO_2 by oxy-combustion leads to irreversible sulphation of the sorbent. The requirement of an air separation unit, consumption of additional fuel, and production of extra CO_2 by oxy-combustion are further drawbacks imposing a considerable penalty on the technology [7]. Current research efforts are focused on the development of innovative techniques to improve the calciner efficiency [8, 9] and recover heat from the solids and gaseous streams leaving it [7, 10, 11].

A major advantage for the industrial competitiveness of the CaL technology is the low cost, wide availability and synergy with the cement industry of natural limestone [12–14]. However, limestone derived CaO suffers a progressive loss of reactivity when subjected to multiple carbonation/calcination cycles, which is a further critical aspect of the CaL technology. CO_2 chemisorption on solid CaO particles for short times occurs mainly in a kinetically-

driven phase which progresses at a fast rate until a 30-50 nm thick layer of $CaCO_3$ is built up on the solid's surface [15, 16]. Further carbonation is controlled by the diffusion of CO_3^{2-} mobile ions and counter-current diffusion of O^{2-} anions through the $CaCO_3$ product layer [17, 18], which takes place at a much lower rate. It is thus thought that the progressive loss of CaO reactivity in short residence times is due to the reduction of the surface area caused by enhanced sintering at the high calcination temperatures needed for sorbent regeneration [19–21]. Multicyclic thermogravimetric analysis (TGA) tests involving calcination temperatures up to 950°C (albeit under low CO_2 partial pressure) show that the multicyclic CaO conversion ($X \equiv$grams of CaO carbonated/grams of CaO initial in each cycle) decays gradually with the cycle number and converges asymptotically to a residual value $X_r \simeq 0.07-0.08$ [19, 22]. On the other hand, experimental observations indicate that the presence of CO_2 at high concentration in the calcination atmosphere leads to a significantly marked drop of conversion [5, 23–26]. In some tests, CaO conversion is seen to decay in just a few cycles to a value of just about 0.05 when the sorbent is regenerated at high CO_2 concentration/high temperature [25, 26]. It has been suggested that other mechanisms may play a role on the loss of multicyclic CaO conversion such as a progressive growth of the regenerated crystal structure along preferential surfaces, which are more stable but less favorable for $CaCO_3$ nucleation [27–29].

A crucial parameter for closely mimicking CaL conditions by means of TGA tests is the heating rate during the transition between carbonation and calcination. The relatively low heating rates achievable by means of common TG furnaces lead to excessively long transitions between these stages (over a few minutes). Under high CO_2 concentration, this gives rise to appreciable recarbonation until the temperature reaches a high enough value (close to 900°C) to shift the reaction towards decarbonation [23]. According to process

simulations [8, 9], the temperature at the bottom of the calciner would be below the target temperature because of the cold flow of solids coming from the carbonator, which may cause certain recarbonation of these solids. However, this transitory recarbonation would last just a few seconds since the temperature is expected to rise quickly at the height of the fuel inlet [8, 9]. The main objective of the present work is to study the influence of limestone crystallinity (modified by different treatments such as milling and thermal annealing) on its CO_2 capture performance in the CaL process at regeneration conditions closely resembling those in practice, which necessarily involve high CO_2 concentration/high temperature in the calciner and quick transitions between the carbonation and calcination stages. The transition between these stages is shortened in our TGA tests to tens of seconds by means of infrared heating, which allows changing the temperature at a very fast and controlled rate. The effect of recarbonation, which has been recently proposed as a feasible technique to mitigate the multicyclic loss of sorbent reactivity [22, 30–32], will be also analyzed.

II. MATERIALS AND METHODS

In our tests we have used a natural limestone of high purity ($CaCO_3$ 99.62%, $SiO_2 <$ 0.05%, $Al_2O_3 <$ 0.05%, MgO 0.24%, Na_2O 0.08%), which was pre-crushed and sieved to a fine particle size, as received from Matagallar quarry (Pedrera, Spain). Volume weighted mean particle size measured by means of a Mastersizer 2000 (Malvern Instruments) is 9.5 μm. Limestone samples were subjected to diverse treatments such as milling and thermal annealing. Milling is a common treatment used in many industrial applications [33–37] leading a high density of structural defects in the solid crystal structure [38], which serves to enhance solid-state diffusion [34]. In our work, milling was carried out in a 100 cm^3 steel jar with 200 tungsten carbide balls (5.5 mm in diameter) operated in a centrifugal

ball-mill (Fritsch Pulverisette 6, centrifugal version, Idar-Oberstein, Germany) where 6.5 g of limestone was milled at 500 rpm for 2 hours (limestone-to-ball mass ratio was set at 1:40). On the other hand, thermal annealing was pursued in our work by subjecting a limestone sample to a pure CO_2 atmosphere at 850°C (50°C below the equilibrium temperature [39]) for 12 h. Since the annealing temperature (850°C) is well above the Tamman temperature (∼533°C), lattice diffusion of ions is greatly enhanced during this treatment, which reduces the density of structural defects in the solid [40]. As opposed to milling, the increase of crystallinity induced by annealing increases the resistance to solid-state diffusion [41, 42].

Carbonation/calcination (car/cal) cycles have been carried out by means of a Q5000IR TG analyzer (TA Instruments), which is based on a furnace heated by infrared halogen lamps and a high sensitivity balance (<0.1 μg) with a minimum baseline dynamic drift (<10 μg). Undesired effects related to mass transfer on the reaction rate have been avoided in our tests by using in all the runs a fixed mass of 10 mg for which these effects may be dismissed as demonstrated elsewhere [43]. Besides, the small particle size selected allows us neglecting any further effect on the reaction rate caused by intra-particle diffusion resistance, which would be noticeable for particles of size larger than about 300 μm [16, 39].

Prior to car/cal cycles the sample was precalcined in-situ by subjecting it to a linear heating program (20°C/min) up to 850°C in air. Subsequent car/cal cycles consisted of 5 min carbonation at 650°C (85% air/15% CO_2 vol/vol) followed by 5 min calcination under 70% CO_2/30% air vol/vol in a range of temperatures between 900°C and 950°C. Carbonation/recarbonation/calcination (car/recar/cal) cycles were carried out by subjecting the sample to a 3 min recarbonation stage (10% air/90% CO_2 vol/vol) at 800°C in between the carbonation and calcination stages. Heating and cooling rates between stages were set to 300°C min^{-1}. Results from TGA tests reported elsewhere [32, 44] in which the sorbents

were regenerated by calcination in air at 850°C will be shown for comparison.

III. EXPERIMENTAL RESULTS AND DISCUSSION

A. Samples characterization

Scanning Electron (SEM) and Scanning Probe Microscopy (SPM) images shown in Fig. 1 demonstrate contrasting effects of milling and thermal annealing on the structure of the solids. Structural damage is clearly appreciable in the milled particles. In contrast, the surfaces of annealed particles appear visibly smoothed. X-Ray diffractograms (XRD) are shown in Fig. 2(a-c). As may be seen, the raw limestone exhibits a high degree of crystallinity (Fig. 2a), which is noticeably decreased by ball milling (Fig. 2b). Conversely, annealing causes a further increase of the degree of crystallinity as expected (Fig. 2c).

Pore size distributions obtained by physisorption analysis (N_2 sorption at 77 K) are plotted in Fig. 2d. It is observed that milling gives rise to a marked increase of the pore population in the whole size interval (2–200 nm). On the other hand, small pores vanish in the annealed sample arguably due to enhanced sintering by lattice diffusion [45] whereas the population of larger pores is increased, which agrees with the general observation that annealing for long time at high temperature leads a notable increase of the size of pores [46, 47]. The pore size distributions obtained for these samples after calcination in a muffle furnace for 30 min (850°C in air) are also shown in Fig. 2d. As may be seen, there is a growth of the population of the smallest pores (2-4 nm), which would be caused by CO_2 leaving the $CaCO_3$ inward skeleton [15]. Remarkably, the distributions obtained for the CaO skeletons resulting from calcination of raw and milled limestones are quite similar. In the domain of pores larger than 4 nm, these distributions are close to the pore size distribution of the

milled limestone, which suggests that the damage caused by milling favors the structural change that accompanies decarbonation. On the other hand, the evolution of the pore size distribution for the annealed sample upon calcination is qualitatively different. In this case, the pore size distribution exhibits a marked displacement towards the region of small pores caused by bulk decarbonation.

B. Carbonation/calcination multicyclic behavior

Figure 3 shows the time evolution of the sorbent weight% during the first cycles of two different car/cal tests in which sorbent regeneration was carried out by calcination at 950°C under 70% vol CO_2 (Fig. 3a) and at 850°C in air (Fig. 3b), respectively. As may be seen, most of carbonation in the 1st cycle (just after precalcination in air) occurs through the kinetically controlled fast phase and up to an extent similar for the three samples. The carbonation reactivity of CaO derived from calcination of limestone in air is mainly correlated to its surface area [15, 21, 48]. As seen above, the CaO skeletons derived from calcination of the raw and milled limestones in air show very similar porosity (Fig. 2d) and BET surface area (6.2 m^2/g and 6.3 m^2/g, respectively). On the other hand, the pore size distribution is shifted towards the small pores (< 6 nm) domain for the annealed limestone derived CaO, whose BET surface area results slightly higher (9.4 m^2/g). However, blockage of very small pores is likely to occur during carbonation in short times [49], which would limit the potentially higher maximum CaO conversion in the fast phase of this sorbent. Anyhow, conversions in the 1st carbonation of the CaO derived from precalcination of the three samples in air are similar as seen in Figs. 3(a-b).

Let us focus on the main subject of the present work, namely the effect of limestone crystal structure on the multicyclic CaO conversion at realistic regeneration conditions. Once

the fast carbonation phase is ended, CaO conversion turns to be controlled by diffusion and should be inversely correlated to CaO crystallite size as recently shown for Ca-based synthetic sorbents [48]. Accordingly, we see in Fig. 3 that carbonation in the diffusion-controlled slow phase is enhanced for the milled sample whereas annealing hinders it. This becomes more apparent in the short transition existing between carbonation and calcination when the samples are regenerated under 70% vol CO_2. The sharp overshoot observed in the weight gain during this transitory period (Fig. 3a) is due to the enhancement of carbonation when the CO_2 % is suddenly increased from 15% vol up to 70% vol and until the temperature reaches the equilibrium temperature ($\sim$870°C in a 70% vol CO_2 atmosphere [39]). According to a recently proposed mechanism for carbonation, $CaCO_3$ would nucleate on the CaO surface forming islands with a critical size determined by surface diffusion [50, 51]. Since surface diffusion becomes noticeable at temperatures close to the Huttig temperature ($T_H \simeq 690$°C for CaO and $T_H \simeq 260$°C for $CaCO_3$ [52]) it would be greatly promoted when the temperature is increased and favored by structural defects, which would enhance the exposition of CaO surface available for accelerated recarbonation in this transitory short period. In contrast, hindered surface diffusion in the annealed solid would hamper recarbonation as seen in Fig. 3a. The correlation between the diffusion-controlled carbonation activity and the original limestone crystallinity persists along successive cycles, which suggests that the effect of pretreatment remains imprinted in the solid crystal structure.

Even though the critical temperature to shift the reaction towards decarbonation in a 70% vol CO_2 atmosphere would be about 870°C [39], a minimum temperature of 950°C was needed in our tests to achieve full decarbonation during the 1st regeneration of the raw limestone derived sorbent, which agrees with observations from pilot-scale [2] and batch fluidized bed [5, 6] tests. We see however that the limestone crystal structure has a significant

effect on the kinetics of decarbonation when the carbonated sorbent is regenerated under high temperature/high CO_2 concentration (Fig. 3a). In analogy with the effect of the crystal structure on diffusion-controlled carbonation, decarbonation is notably enhanced for the sorbent derived from milled limestone whereas it is otherwise for the sorbent derived from the annealed limestone. Note however that the effect of crystallinity on decarbonation is only observed when calcination is carried out under high CO_2 partial pressure (Fig. 3a). There is no appreciable effect in the case of regeneration by calcining in air (Fig. 3a). This issue might be linked to the dissimilarity between the mechanisms that govern decarbonation of $CaCO_3$ depending on the CO_2 partial pressure. While decarbonation in air would occur via fast and irreversible desorption of CO_2, the ruling mechanism at high CO_2 partial pressure would consist of a dynamic and reversible adsorption/desorption of CO_2 in the solid [39, 53–56]. Our results suggest that this complex process is essentially influenced by the resistance to diffusion in the solid structure. Thus, it would be favored by the structural damage caused by milling whereas it would be notably hampered by thermal annealing.

A further interesting feature illustrated by Figs. 3(a-b) regards the activity of the regenerated sorbent as affected by the calcination atmosphere. The thermograms show that the carbonation activity in the fast phase is severely hampered when the sorbent is regenerated under a high CO_2 partial pressure atmosphere (Fig. 3a). Besides, the rate of diffusion-controlled carbonation is notably promoted as compared with regeneration in air (Fig. 3b). In fact, it is seen that diffusion-controlled carbonation yields a significant contribution to the overall CaO conversion in the 5 min carbonation stage. For example, CaO conversion in the diffusion-controlled phase of the 3rd cycle is almost twice conversion in the fast phase for the milled limestone derived sorbent. This observation contrasts with the common believe that most of CaO conversion in practice would be due to carbonation in the fast phase, which is

indeed the case for the sorbents regenerated in air as seen in Fig. 3b. Our results suggest otherwise: carbonation in the diffusion-controlled phase may be a significant contribution to conversion in short residence times when the sorbent is regenerated at high CO_2 partial pressure. In the practical application, the solids in the carbonator are fluidized with the incoming flue gas. After being separated from the gas they are transferred along a standpipe to a loop seal from which a part of the solids is circulated to the calciner for regeneration and the rest is recirculated back to the carbonator [9]. Solids recirculation in the carbonator serves to increase their residence time, which would be ideally in the range 1-5 minutes [4]. The enhanced rate of carbonation in the diffusion-controlled phase evidenced by our results suggest that it would be advisable to increase the residence time in the carbonator before the solids are transported to the calciner for regeneration, which entails an irreversible loss of conversion in the next cycle.

In the light of the above results, it may be envisaged that a potential benefit of using poorly crystalline limestone in the CaL technology would be the possibility of lowering down the calcination temperature. This is demonstrated by the thermograms shown in Fig. 4 derived from multicyclic tests in which sorbent regeneration was carried out under 70% CO_2 at 900°C. As may be observed, decarbonation is slow and incomplete at this insufficiently high temperature for regeneration of the sorbent derived from raw limestone. The scenario becomes even more adverse for the annealed sample with a higher crystallinity that severely hampers decarbonation. On the other hand, the sorbent derived from milled limestone exhibits fast and complete decarbonation at 900°C in short times from the 1st cycle.

C. Carbonation/recarbonation/calcination multicyclic behavior

Previous works [22, 30, 32] have demonstrated that a purposely introduced recarbonation stage at high temperature/high CO_2 concentration between carbonation and calcination leads to a reactivation of the sorbent albeit in the multicyclic TGA tests carried out in those studies the sorbents were regenerated by calcination in a low CO_2 partial pressure environment. Let us closely look at the effect of recarbonation as determined by limestone crystallinity when regeneration is carried out at high CO_2 partial pressure. Figure 5 shows the thermograms derived from car/recar/cal multicyclic tests. As expected from the above analysis on the transitory recarbonation observed in car/cal tests, crystallinity has a notable effect on conversion in the purposely introduced recarbonation stage of these tests, being it significantly intensified for the milled sample whereas it is the opposite for the annealed limestone. Yet, in contradiction with results from car/recar/cal tests reported elsewhere [22, 32, 57] in which sorbent regeneration was carried out in air, our results show that recarbonation does not lead to a mitigation of the decay of CaO conversion in the carbonation stage. Actually, recarbonation slows down decarbonation during regeneration at high CO_2 partial pressure and 900°C (Fig. 5b). Note in fact that the annealed sample shows a higher decarbonation rate at 900°C than the raw limestone (Fig. 5b), which can be explained by its lower susceptibility to recarbonation due to its enhanced crystallinity. Moreover, the carbonation reactivity of the sorbent regenerated under high CO_2 concentration after recarbonation suffers an even deeper drop as will be shown next further detail.

D. Multicyclic CaO conversion

Data on CaO conversion at the end of the carbonation stage X_N are plotted in Fig. 6 as a function of the cycle number N for multicyclic tests in which decarbonation at high CO_2 partial pressure was complete from the 1st regeneration. Data from multicyclic tests in which sorbent regeneration was carried out in air are shown for comparison.

A main observation is the drastic drop of conversion caused by the presence of CO_2 at high concentration in the calcination atmosphere (note the vertical log scale). The decay of conversion is however lessened at the reduced calcination temperature (900°C) for the milled sample, which exhibits after 20 cycles a value of conversion almost twice that of the raw limestone (necessarily regenerated at 950°C to attain complete decarbonation).

In regards to recarbonation, its detrimental effect is clearly illustrated for all the tests carried out in which sorbent regeneration was carried out at high CO_2 partial pressure. Moreover, the harmful effect of recarbonation becomes more apparent for the milled sample because enhanced diffusion intensifies it as seen above. Note in Fig. 6 that the opposed effect of recarbonation, mitigating the loss of CaO conversion (previously reported [22, 30, 32]), if the sorbents are regenerated in air is reproduced by tests carried out in our work, which emphasizes the importance of closely mimicking CaL conditions for extracting valuable information to scale-up the process from lab-scale multicyclic tests.

E. Improvement of the CaL technology efficiency

It has been estimated from process simulations [58] that the energy demand in the calciner may represent a fraction near half the total energy required in the CaL technology, and it could be even higher if the adverse effect of sorbent regeneration under high CO_2

concentration was considered. Thus, attaining full decarbonation at the lowest possible calcination temperature would serve to boost the industrial competitiveness of the technology, mainly by avoiding the amount of coal and oxygen needed for oxy-combustion and reducing the extra CO_2 generated [8]. Yet, process simulations [3] show that the calciner efficiency to achieve full decarbonation only becomes sufficiently high at temperatures close to 950°C and is severely hampered when the temperature is decreased below 900°C. As seen in our work, decarbonation of raw limestone is too slow at temperatures below 950°C under high CO_2 partial pressure. Our results indicate however that the use of natural limestones with decreased crystallinity speeds up decarbonation, which can be fully attained in short residence times at 900°C. According to process simulations [7, 59], the ratio of the mass of coal required for oxy-combustion to the mass of CO_2 captured would be decreased from 0.45 at 950°C to 0.4 at 900°C [7]. Besides of the reduction of coal and oxygen needs in the calciner, the improvement of reactivity of the sorbent regenerated at decreased calcination temperature would bring about a notable redction of the cost of CO_2 avoided. For relative increments of CaO conversion comparable to the observed in our study by using milled limestone, the reduction of CO_2 avoided could be estimated between 1.5 and 3 €/tonne depending on the CaO/CO_2 molar ratio [12]. Even though in our study limestone crystallinity has been modified by applying diverse pretreatments it may be argued that the degree of crystallinity of the limestone to be used in the practical process should be an important parameter to be considered when assessing the scaled-up process efficiency. Ideally, low crystalline limestones should be selected in practice, which would serve to decrease the calcination temperature and mitigate the decay of sorbent capture capacity. Otherwise, the use of limestones of high crystallinity should be avoided.

IV. ACKNOWLEDGEMENTS

This work was supported by the Andalusian Regional Government Junta de Andalucia (contracts FQM-5735 and TEP-7858), Spanish Government Agency Ministerio de Economia y Competitividad and FEDER funds (contracts FIS2011-25161 and CTQ2011-27626). One of the authors (PESJ) is supported by the Juan de la Cierva program of the Spanish Ministerio de Economia y Competitividad. We gratefully acknowledge the Microscopy, Functional Characterization and X-ray services of the Innovation, Technology and Research Center of the University of Seville (CITIUS). The help of Dr. M.A.S. Quintanilla with the SPM analysis is warmly appreciated.

V. REFERENCES

[1] J. Blamey, E. J. Anthony, J. Wang, and P. S. Fennell, "The calcium looping cycle for large-scale CO_2 capture," *Prog. Energ. Combust. Sci.*, vol. 36, no. 2, pp. 260–279, 2010.

[2] B. Arias, M. Diego, J. Abanades, M. Lorenzo, L. Diaz, D. Martinez, J. Alvarez, and A. Sanchez-Biezma, "Demonstration of steady state CO_2 capture in a 1.7 MWth calcium looping pilot," *International Journal of Greenhouse Gas Control*, vol. 18, pp. 237 – 245, 2013.

[3] I. Martinez, G. Grasa, R. Murillo, B. Arias, and J. Abanades, "Modelling the continuous calcination of $CaCO_3$ in a Ca-looping system," *Chemical Engineering Journal*, vol. 215–216, pp. 174–181, 2013.

[4] A. Charitos, N. Rodriguez, C. Hawthorne, M. Alonso, M. Zieba, B. Arias, G. Kopanakis, G. Scheffknecht, and J. C. Abanades, "Experimental validation of the Calcium Looping CO_2

capture process with two circulating fluidized bed carbonator reactors," *Industrial & Engineering Chemistry Research*, vol. 50, no. 16, pp. 9685–9695, 2011.

[5] R. T. Symonds, D. Y. Lu, V. Manovic, and E. J. Anthony, "Pilot-scale study of CO_2 capture by cao-based sorbents in the presence of steam and SO_2," *Industrial & Engineering Chemistry Research*, vol. 51, no. 21, pp. 7177 – 7184, 2012.

[6] A. Coppola, F. Scala, P. Salatino, and F. Montagnaro, "Fluidized bed calcium looping cycles for CO_2 capture under oxy-firing calcination conditions: Part 1. assessment of six limestones," *Chemical Engineering Journal*, vol. 231, pp. 537 – 543, 2013.

[7] A. Martinez, Y. Lara, P. Lisbona, and L. M. Romeo, "Operation of a cyclonic preheater in the Ca-looping for CO_2 capture," *Environmental Science & Technology*, vol. 47, no. 19, pp. 11335–11341, 2013.

[8] J. Ylatalo, J. Parkkinen, J. Ritvanen, T. Tynjala, and T. Hyppanen, "Modeling of the oxy-combustion calciner in the post-combustion calcium looping process," *Fuel*, vol. 113, pp. 770–779, 2013.

[9] J. Ylatalo, J. Ritvanen, T. Tynjala, and T. Hyppanen, "Model based scale-up study of the calcium looping process," *Fuel*, vol. 115, pp. 329–337, 2014.

[10] A. Martinez, Y. Lara, P. Lisbona, and L. M. Romeo, "Energy penalty reduction in the calcium looping cycle," *International Journal of Greenhouse Gas Control*, vol. 7, pp. 74 – 81, 2012.

[11] Y. Lara, P. Lisbona, A. Martnez, and L. M. Romeo, "Design and analysis of heat exchanger networks for integrated Ca-looping systems," *Applied Energy*, vol. 111, pp. 690 – 700, 2013.

[12] L. M. Romeo, Y. Lara, P. Lisbona, and A. Martinez, "Economical assessment of competitive enhanced limestones for CO_2 capture cycles in power plants," *Fuel Processing Technology*, vol. 90, no. 6, pp. 803 – 811, 2009.

[13] N. Rodriguez, M. Alonso, J. C. Abanades, A. Charitos, C. Hawthorne, G. Scheffknecht, D. Y. Lu, and E. J. Anthony, "Comparison of experimental results from three dual fluidized bed test facilities capturing CO_2 with CaO," *Energy Procedia*, vol. 4, pp. 393 – 401, 2011.

[14] M. C. Romano, I. Martinez, R. Murillo, B. Arstad, R. Blom, D. C. Ozcan, H. Ahn, and S. Brandani, "Process simulation of Ca-looping processes: review and guidelines," *Energy Procedia*, vol. 37, pp. 142 – 150, 2013.

[15] R. Barker, "Reversibility of the reaction $CaCO_3$ =CaO+CO_2," *J. Appl. Chem. Biotechnol.*, vol. 23, pp. 733 – 742, 1973.

[16] G. Grasa, R. Murillo, M. Alonso, and J. C. Abanades, "Application of the random pore model to the carbonation cyclic reaction," *AIChE J.*, vol. 55, no. 5, pp. 1246–1255, 2009.

[17] S. K. Bhatia and D. D. Perlmutter, "Effect of the product layer on the kinetics of the CO_2-lime reaction," *AIChE Journal*, vol. 29, no. 1, pp. 79–86, 1983.

[18] Z. Sun, S. Luo, P. Qi, and L.-S. Fan, "Ionic diffusion through calcite ($CaCO_3$) layer during the reaction of cao and CO_2," *Chemical Engineering Science*, vol. 81, pp. 164 – 168, 2012.

[19] G. S. Grasa and J. C. Abanades, "CO_2 capture capacity of CaO in long series of carbonation/calcination cycles," *Ind. Eng. Chem. Res.*, vol. 45, no. 26, pp. 8846–8851, 2006.

[20] A. I. Lysikov, A. N. Salanov, and A. G. Okunev, "Change of CO_2 carrying capacity of CaO in isothermal recarbonation-decomposition cycles," *Ind. Eng. Chem. Res.*, vol. 46, pp. 4633 – 4638, 2007.

[21] J. M. Valverde, "A model on the CaO multicyclic conversion in the Ca-looping process," *Chemical Engineering Journal*, vol. 228, pp. 1195–1206, 2013.

[22] B. Arias, G. S. Grasa, M. Alonso, and J. C. Abanades, "Post - combustion calcium looping process with a highly stable sorbent activity by recarbonation," *Energy Environ. Sci.*, vol. 5,

pp. 7353 – 7359, 2012.

[23] D. Y. Lu, R. W. Hughes, E. J. Anthony, and V. Manovic, "Sintering and reactivity of $CaCO_3$-based sorbents for in situ CO_2 capture in fluidized beds under realistic calcination conditions," *J. Environ. Eng.*, vol. 135, no. 6, pp. 404–410, 2009.

[24] V. Manovic, J.-P. Charland, J. Blamey, P. S. Fennell, D. Y. Lu, and E. J. Anthony, "Influence of calcination conditions on carrying capacity of CaO-based sorbent in CO_2 looping cycles," *Fuel*, vol. 88, pp. 1893–1900, 2009.

[25] J. Valverde, P. Sanchez-Jimenez, and L. Perez-Maqueda, "Calcium-looping for post-combustion CO_2 capture. on the adverse effect of sorbent regeneration under CO_2," *Applied Energy*, vol. 126, pp. 161–171, 2014.

[26] J. M. Valverde, P. E. Sanchez-Jimenez, and L. A. Perez-Maqueda, "Effect of heat pretreatment/recarbonation in the Ca-looping process at realistic calcination conditions," *Energy & Fuels*, 2014.

[27] R. Besson, M. R. Vargas, and L. Favergeon, "CO_2 adsorption on calcium oxide: An atomic-scale simulation study," *Surface Science*, vol. 606, no. 3 4, pp. 490 – 495, 2012.

[28] R. Besson and L. Favergeon, "Atomic - scale study of calcite nucleation in calcium oxide," *The Journal of Physical Chemistry C*, vol. 117, no. 17, pp. 8813 – 8821, 2013.

[29] J. P. Allen, A. Marmier, and S. C. Parker, "Atomistic simulation of surface selectivity on carbonate formation at calcium and magnesium oxide surfaces," *The Journal of Physical Chemistry C*, vol. 116, no. 24, pp. 13240 – 13251, 2012.

[30] G. Grasa, I. Martnez, M. E. Diego, and J. C. Abanades, "Determination of CaO carbonation kinetics under recarbonation conditions," *Energy & Fuels*, doi:10.1021/ef500331t.

391 [31] M. E. Diego, B. Arias, G. S. Grasa, and J. C. Abanades, "Design of a novel fluidized bed
392 reactor to enhance sorbent performance in CO_2 capture systems using CaO," *Industrial &*
393 *Engineering Chemistry Research*, doi:10.1021/ie500630p.
394 [32] J. M. Valverde, P. E. Sanchez Jimenez, and L. A. Perez Maqueda, "High and stable CO_2
395 capture capacity of natural limestone at Ca-looping conditions by heat pretreatment and
396 recarbonation synergy," *Fuel*, vol. 123, pp. 79–85, 2014.
397 [33] Q. Zhang, E. Kasai, H. Mimura, and F. Saito, "Effect of dry grinding on ion-exchange char-
398 acteristics of synthetic mordenite," *Advanced Powder Technology*, vol. 5, no. 3, pp. 289 – 296,
399 1994.
400 [34] P. Heitjans and S. Indris, "Fast diffusion in nanocrystalline ceramics prepared by ball milling,"
401 *Journal of Materials Science*, vol. 39, no. 16-17, pp. 5091–5096, 2004.
402 [35] P. E. Sanchez-Jimenez, L. A. Perez-Maqueda, M. J. Dianez, A. Perejon, and J. M. Criado,
403 "Mechanochemical preparation of $BaTiO_3Ni$ nanocomposites with high dielectric constant,"
404 *Composite Structures*, vol. 92, no. 9, pp. 2236–2240, 2010.
405 [36] A. Perejon, N. Murafa, P. E. Sanchez-Jimenez, J. M. Criado, J. Subrt, M. J. Dianez, and L. A.
406 Perez-Maqueda, "Direct mechanosynthesis of pure $BiFeO_3$ perovskite nanoparticles: reaction
407 mechanism," *J. Mater. Chem. C*, vol. 1, pp. 3551–3562, 2013.
408 [37] A. Perejon, N. Maso, A. R. West, P. E. Sanchez-Jimenez, R. Poyato, J. M. Criado, and L. A.
409 Perez-Maqueda, "Electrical properties of stoichiometric $BiFeO_3$ prepared by mechanosynthesis
410 with either conventional or spark plasma sintering," *Journal of the American Ceramic Society*,
411 vol. 96, no. 4, pp. 1220–1227, 2013.
412 [38] J. S. Forrester, H. J. Goodshaw, E. H. Kisi, G. J. Suaning, and J. S. Zobec, "Effect of
413 mechanical milling on the sintering behaviour of alumina," *J. Aust. Ceram. Soc.*, vol. 44,

no. 1, pp. 47 – 52, 2008.

[39] F. Garcia-Labiano, A. Abad, L. de Diego, P. Gayan, and J. Adanez, "Calcination of calcium-based sorbents at pressure in a broad range of CO_2 concentrations," *Chemical Engineering Science*, vol. 57, no. 13, pp. 2381 – 2393, 2002.

[40] M. Liu and B. Evans, "Dislocation recovery kinetics in single-crystal calcite," *Journal of Geophysical Research: Solid Earth*, vol. 102, no. B11, pp. 24801–24809, 1997.

[41] A. K. Kronenberg, R. A. Yund, and B. J. Giletti, "Carbon and oxygen diffusion in calcite: Effects of Mn content and PH2O," *Physics and Chemistry of Minerals*, vol. 11, no. 3, pp. 101–112, 1984.

[42] T. F. Anderson, "Self-diffusion of carbon and oxygen in calcite by isotope exchange with carbon dioxide," *Journal of Geophysical Research*, vol. 74, no. 15, pp. 3918–3932, 1969.

[43] M. Alonso, Y. Criado, J. Abanades, and G. Grasa, "Undesired effects in the determination of CO_2 carrying capacities of CaO during TG testing," *Fuel*, pp. –, 2013.

[44] J. Valverde, P. Sanchez-Jimenez, L. Perez-Maqueda, M. Quintanilla, and J. Perez-Vaquero, "Role of crystal structure on capture by limestone derived CaO subjected to carbonation/recarbonation/calcination cycles at Ca-looping conditions," *Applied Energy*, vol. 125, pp. 264 – 275, 2014.

[45] D. R. Glasson, "Reactivity of lime and related oxides. xvi. sintering of lime," *J. Appl. Chem.*, vol. 17, p. 91 96, 1967.

[46] D. Z. Fang, C. C. Striemer, T. R. Gaborski, J. L. McGrath, and P. M. Fauchet, "Methods for controlling the pore properties of ultra-thin nanocrystalline silicon membranes," *Journal of Physics: Condensed Matter*, vol. 22, no. 45, p. 454134, 2010.

[47] T. Tao, A. M. Glushenkov, Q. Chen, H. Hu, D. Zhou, H. Zhang, M. Boese, S. Liu, R. Amal, and Y. Chen, "Porous TiO_2 with a controllable bimodal pore size distribution from natural ilmenite," *CrystEngComm*, vol. 13, pp. 1322–1327, 2011.

[48] A. Akgsornpeak, T. Witoon, T. Mungcharoen, and J. Limtrakul, "Development of synthetic CaO sorbents via CTAB-assisted solgel method for CO_2 capture at high temperature," *Chemical Engineering Journal*, vol. 237, pp. 189 – 198, 2014.

[49] D. Alvarez and J. C. Abanades, "Pore-size and shape effects on the recarbonation performance of calcium oxide submitted to repeated calcination/recarbonation cycles," *Energy and Fuels*, vol. 19, pp. 270–278, 2005.

[50] Z.-S. Li, F. Fang, X.-Y. Tang, and N.-S. Cai, "Effect of temperature on the carbonation reaction of CaO with CO_2," *Energy & Fuels*, vol. 26, no. 4, pp. 2473–2482, 2012.

[51] Z. Li, H. Sun, and N. Cai, "Rate equation theory for the carbonation reaction of cao with CO_2," *Energy & Fuels*, vol. 26, no. 7, pp. 4607–4616, 2012.

[52] A. M. Kierzkowska, R. Pacciani, and C. R. Müller, "CaO-based CO_2 sorbents: From fundamentals to the development of new, highly effective materials," *ChemSusChem*, vol. 6, no. 7, pp. 1130–1148, 2013.

[53] E. P. Hyatt, I. B. Cutler, and M. E. Wadsworth, "Calcium carbonate decomposition in carbon dioxide atmosphere," *Journal of the American Ceramic Society*, vol. 41, no. 2, pp. 70–74, 1958.

[54] D. Beruto, L. Barco, and A. W. Searcy, "CO_2-catalyzed surface area and porosity changes in high-surface-area CaO aggregates," *Journal of the American Ceramic Society*, vol. 67, no. 7, pp. 512–516, 1984.

[55] J. Khinast, G. Krammer, C. Brunner, and G. Staudinger, "Decomposition of limestone: The influence of CO_2 and particle size on the reaction rate," *Chemical Engineering Science*, vol. 51,

459 no. 4, pp. 623–634, 1996.

460 [56] D. Beruto, A. W. Searcy, and M. G. Kim, "Microstructure, kinetic, structure, thermodynamic
461 analysis for calcite decomposition: free-surface and powder bed experiments," *Thermochimica*
462 *Acta*, vol. 424, no. 1 2, pp. 99 – 109, 2004.

463 [57] C. Salvador, D. Lu, E. Anthony, and J. Abanades, "Enhancement of CaO for CO_2 capture in
464 an FBC environment," *Chemical Engineering Journal*, vol. 96, no. 1 3, pp. 187 – 195, 2003.

465 [58] N. Rodriguez, M. Alonso, G. Grasa, and J. C. Abanades, "Heat requirements in a calciner
466 of $CaCO_3$ integrated in a CO_2 capture system using CaO," *Chemical Engineering Journal*,
467 vol. 138, no. 1–3, pp. 148–154, 2008.

468 [59] M. C. Romano, "Modeling the carbonator of a Ca-looping process for CO_2 capture from power
469 plant flue gas," *Chemical Engineering Science*, vol. 69, pp. 257 – 269, 2012.

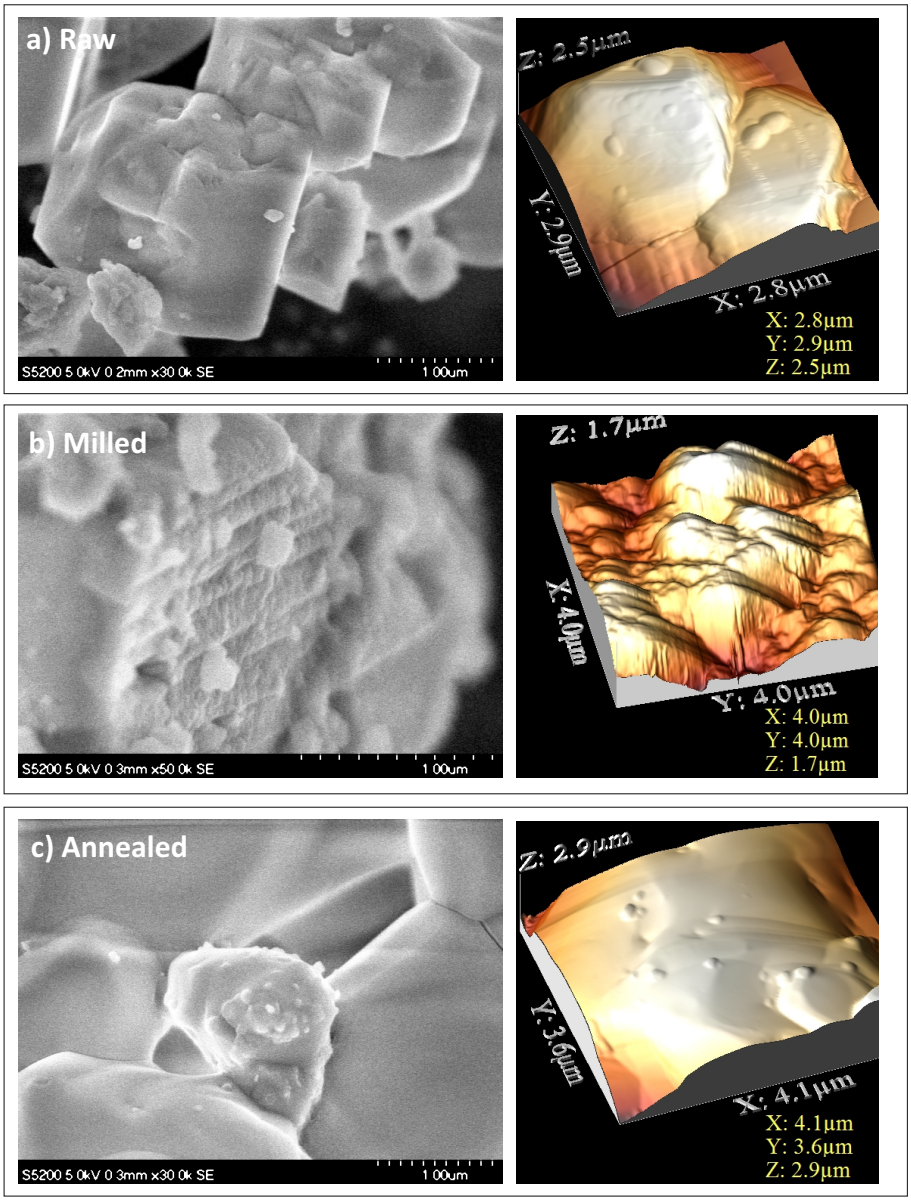

FIG. 1. Scanning Electron Microscopy (SEM) and 3D Scanning Probe Microscope (SPM) images of limestone particles from raw (a), milled (b) and thermally annealed (c) samples. SEM analysis was made by using a HITACHI Ultra High-Resolution S-5200 equipment. SPM images were obtained by using a Molecular Imaging Pico Plus system provided with AppNano ACT silicon tapping-mode rectangular cantilevers.

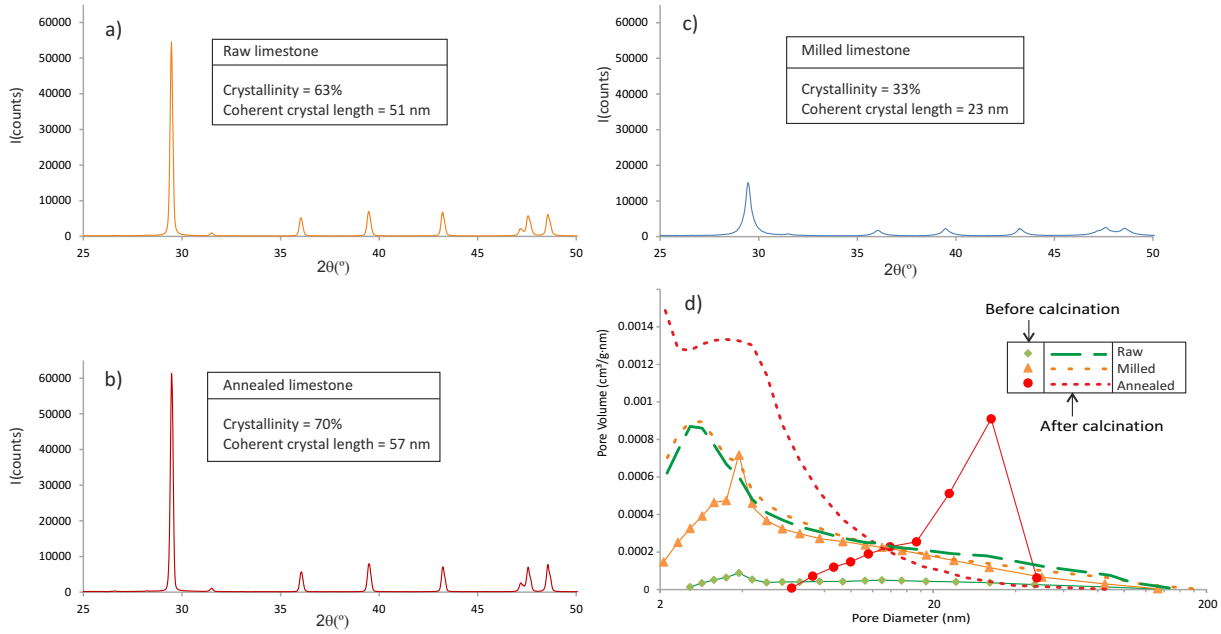

FIG. 2. X-Ray diffractograms (XRD) measured for raw (a), milled (b) and annealed (c) limestone samples. The insets indicate values of the crystallinity % (determined by XRD pattern analysis) and crystallite size, which is obtained from the Scherrer equation and X-ray line broadening FWHM (full width at half maximum intensity) of the most intense (211) peak ($2\theta \simeq 29.5°$). d) BJH desorption pore volume distributions for these samples before and after calcination for 30 min in a muffle furnace under air.

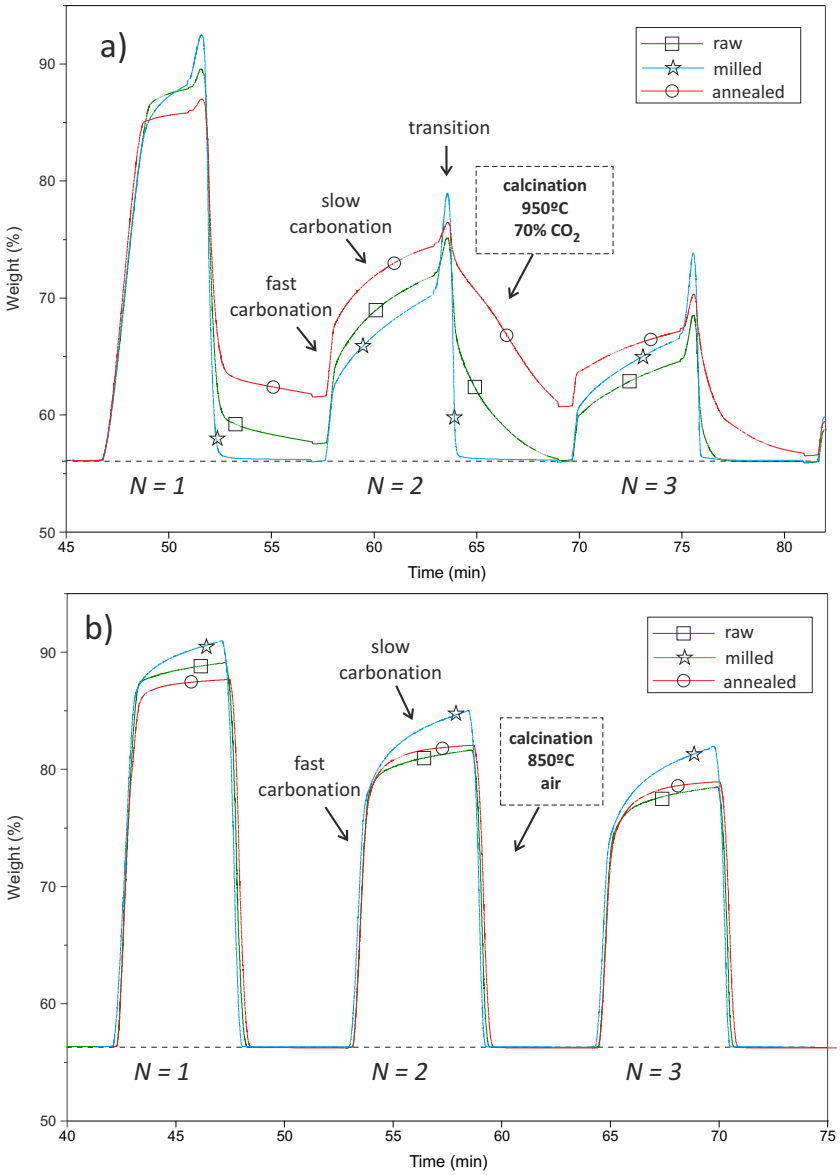

FIG. 3. Time evolution of sorbent weight % during carbonation/calcination cycles for samples of raw, milled and annealed limestones. Carbonation at 650°C for 5 min (15% CO_2/85% air vol/vol). Calcination for 5 min at 950°C (70% CO_2/30% air vol/vol) in (a) and at 850°C (air) in (b). Fast and slow phases in the carbonation stage and the calcination stage are indicated for the second cycle. Note in (a) the sharp increase in the weight % at the end of the carbonation stage, which is indicative of a transitory recarbonation that occurs between carbonation and calcination when the CO_2 % is suddenly increased and until the temperature reaches a high enough value ($\sim$ 870°C) for decarbonation.

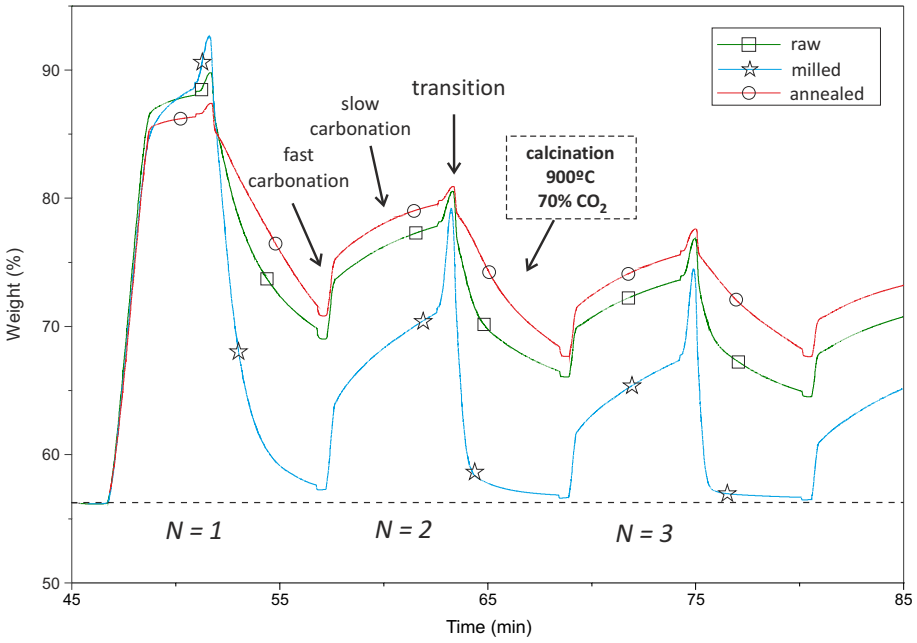

FIG. 4. Time evolution of sorbent weight % during carbonation/calcination cycles for samples of raw, milled and annealed limestones. Carbonation at 650°C for 5 min (15% CO_2/85% air vol/vol). Calcination for 5 min at 900°C (70% CO_2/30% air vol/vol).

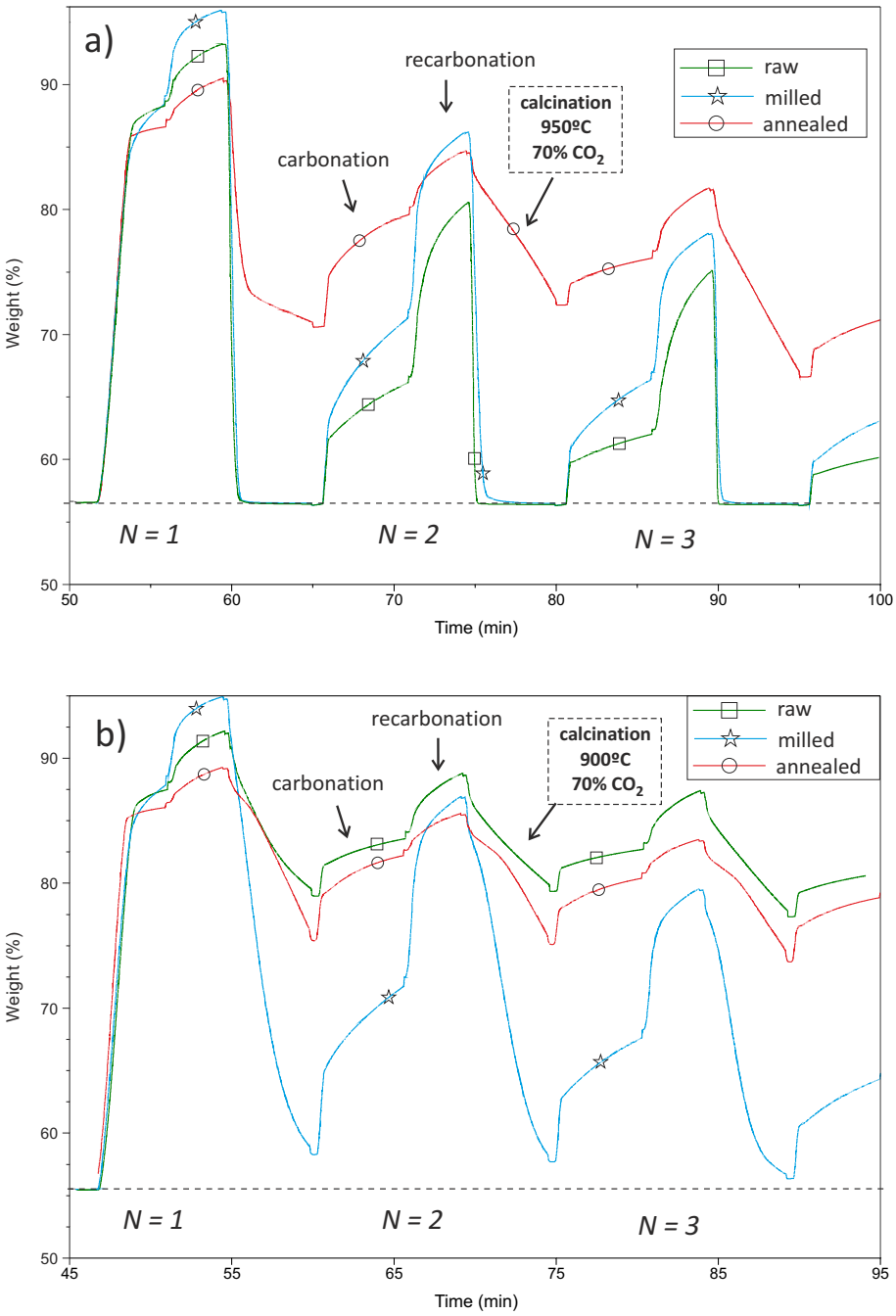

FIG. 5. Time evolution of sorbent weight % during carbonation/recarbonation/calcination cycles for samples of raw, milled and annealed limestones. Carbonation at 650°C for 5 min (15% CO_2/85% air vol/vol), recarbonation at 800°C for 3 min (90% CO_2/10% air vol/vol) and calcination for 5 min (70% CO_2/30% air vol/vol) at 950°C (a) and 900°C (b). Carbonation, recarbonation and calcination stages are indicated for the 2nd cycle.

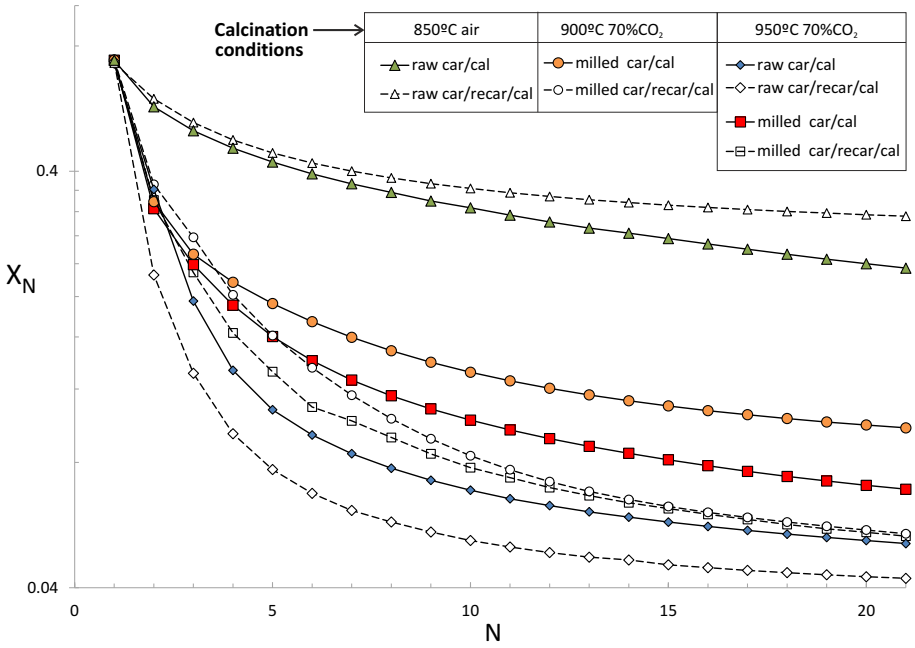

FIG. 6. CaO conversion at the end of the carbonation stage as a function of the cycle number for raw and milled limestone samples subjected carbonation/calcination (car/cal) and carbonation/recarbonation/calcination (car/recar/cal) cycles at different calcination conditions for regeneration (as indicated) leading to complete decarbonation from the 1st cycle. Note the vertical log scale.